La radiologia medica (2018) 123:710–718
https://doi.org/10.1007/s11547-018-0897-0

PAEDIATRIC RADIOLOGY

Evaluation of parotid glands in healthy children and adolescents using shear wave elastography and superb microvascular imaging

Emine Caliskan[1] · Mehmet Ozturk[2] · Zuhal Bayramoglu[1] · Rana Gunoz Comert[3] · Ibrahim Adaletli[1]

Received: 15 November 2017 / Accepted: 20 April 2018 / Published online: 30 April 2018
© Italian Society of Medical Radiology 2018

Abstract

Objectives We aim to determine parotid gland elasticity values from healthy children and adolescents using shear wave elastography (SWE). We also define the degree of vascularity using superb microvascular imaging (SMI), power Doppler (PD), and color Doppler (CD) and compare SMI with CD and PD.

Materials and methods A total of 100 cases, comprising 50 girls and 50 boys, with ages ranging from 3 to 17 years were included in this prospective study. SWE, SMI, PD, and CD measurements were taken from both parotid glands, and the relationships with sex, age, and body mass index (BMI) were determined. The SMI was compared with the PD and CD.

Results The median elasticity values measured with SWE were 8.37 ± 2.09 kPa and 1.68 ± 0.26 m/s on the right and 8.33 ± 2.04 kPa and 1.69 ± 0.26 m/s on the left. There were significant positive correlations present for those aged below and above 10 years and for BMI with elasticity values. The median vascular spot numbers measured using SMI, PD, and CD were 5 ± 1.70, 3.5 ± 1.45, and 2 ± 1.1 on the right and 4 ± 1.7, 4 ± 1.43, and 2 ± 1.05 on the left, respectively. The median values obtained with SMI were significantly higher than the median values obtained with both PD and CD.

Conclusion This study determined the reference SWE, SMI, PD, and CD values for normal parotid glands in healthy children and adolescents. Elasticity values were affected by age and BMI. There was no correlation between vascularity values and age, sex, or BMI. SMI provided more detailed information about vascularity compared with the other methods.

Keywords Children · Color Doppler · Shear wave elastography · Superb microvascular imaging · Parotid gland · Power Doppler

Introduction

Ultrasound elastography is a noninvasive method used to measure the stiffness of tissue—that is, it can obtain a quantitative estimation of the elasticity of different tissues. The earliest developed methods were strain elastography (SE) and acoustic radiation force impulse (ARFI) techniques. The use of shear wave elastography (SWE) has begun to attract more attention in recent years because it is less operator dependent and is easy to apply. The elasticity of tissue in an organ is measured in kiloPascals (kPa) or as shear wave velocity (meters/second; m/s). Tissue elasticity measurements may be beneficial for the identification and treatment of a variety of diseases. As a result, normal elasticity values for the parotid gland may be a marker for diagnosis of infectious diseases like parotitis, inflammatory diseases like juvenile Sjogren syndrome, and neoplastic diseases like lymphoma. Measurements taken with different devices and techniques may provide different values [1, 2]. Additionally, the

✉ Emine Caliskan
eminecaliskanrad@gmail.com

Mehmet Ozturk
drmehmet2121@gmail.com

Zuhal Bayramoglu
incezuhal@yahoo.com

Rana Gunoz Comert
rgcomert@gmail.com

Ibrahim Adaletli
iadaletli@yahoo.com

[1] Department of Pediatric Radiology, Istanbul Faculty of Medicine, Turgut Ozal Street, Fatih, 34063 Istanbul, Turkey

[2] Department of Radiology, Faculty of Medicine, Selcuk University, Alaeddin Keykubat Yerleşkesi, kademi Mah. Yeni Istanbul Street. No:369, Konya, Turkey

[3] Department of Radiology, Istanbul Faculty of Medicine, Turgut Ozal Street, Fatih, Istanbul, Turkey

normal values for the same organ may vary with age or BMI [3, 4]. In the literature, the reference values for various tissues (e.g., liver, spleen, thyroid, breast, muscle and tendon, and kidney) in adults and children have been reported using different devices that employ SE, ARFI, or SWE techniques [5–7]. Though the normal SWE elasticity values for parotid gland tissue have been defined in previous studies, these studies only include the adult population [8, 9]. Gungor et al. [10] published a study defining the normal elasticity values for the parotid gland in pediatric patients using SE; however, to the best of our knowledge, there is no study available that has determined the normal elasticity values with SWE.

The use of Doppler methods for the parotid gland is important in diffuse diseases and tumors [11]. As in adults, increased or reduced tissue vascularity of the parotid gland in children may be helpful in identifying infectious, autoimmune, or neoplastic diseases [12]. With this aim, color Doppler (CD) and power Doppler (PD) methods have been used for many years. The superb microvascular imaging (SMI) technique is a new Doppler method that is able to image much thinner vascular structures [13]. Only a few studies have been published using the SMI technique for liver, kidney, and testis in children [14–16]. However, no study has measured or determined the normal vascularity of parenchyma using the SMI technique for normal parotid glands in children.

The aim of our study is to investigate elasticity values with SWE for parotid gland parenchyma in healthy tissue and to define the degree of vascularity using SMI, PD, and CD techniques. We will also investigate correlations with age, sex, and BMI and compare the vascularity parameters found with the SMI, CD, and PD methods.

Materials and methods

Study subjects and design

This prospective study evaluated 100 pediatric cases (age interval 3–17 years; mean 10.14 ± 3.74), comprising 50 boys and 50 girls, from October 2017 to November 2017 after receiving approval from a local clinical research ethics committee. Before elastography and Doppler investigations were performed, informed consent was obtained from the parents of all cases who accepted participation. Children and adolescents with no medical history, parotid gland pathology, or systemic diseases that may affect the parotid and with homogeneous parenchyma were included in the study. Exclusion criteria were age younger than 3 years, insufficient cooperation, rejecting participation in the study, fever during evaluation, acute parotitis, and tumor, trauma, and surgical history related to the parotid gland. All cases included in the study had sufficient image quality and employed an appropriate technique, so no case was excluded from the study.

Elastography and Doppler measurements were completed by common consensus between two experienced pediatric radiologists with more than 2 years of elastography experience. All measurements were taken with an Aplio 500 Platinum ultrasound device (Toshiba Medical Systems, Japan) with a high-frequency linear probe (frequency range 5–14 MHz). Cases were divided into subgroups, including below and above the age of 10 (children and adolescents, respectively) and girls and boys. The body weight and height were measured and BMI was calculated for each of the cases. Sex, age, and BMI values were compared with elasticity and Doppler values. The SMI, CD, and PD methods were compared with each other.

SWE technique

The ultrasound technique was applied with children lying calm and motionless in the supine position, with the head turned to the side that was opposite of the investigated parotid gland (Fig. 1). Sufficient ultrasound gel was used during elasticity measurements. While obtaining the images, pressure was not applied to the probe, and care was taken that the operator's hand was not moving. In split-screen mode, the 2D-SWE map (left side) and quality mode (right side) were examined (Fig. 2). The quality mode, which is identified as the propagation mode (arrival time contour), is

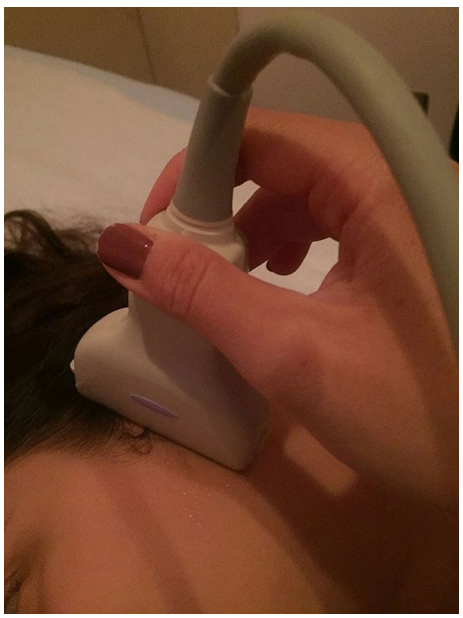

Fig. 1 Shear wave elastography and Doppler techniques were performed while each child remained calm and motionless with their head turned to the side that was opposite of the investigated parotid gland. The ultrasound operator's hand was motionless, and no pressure was applied to the probe

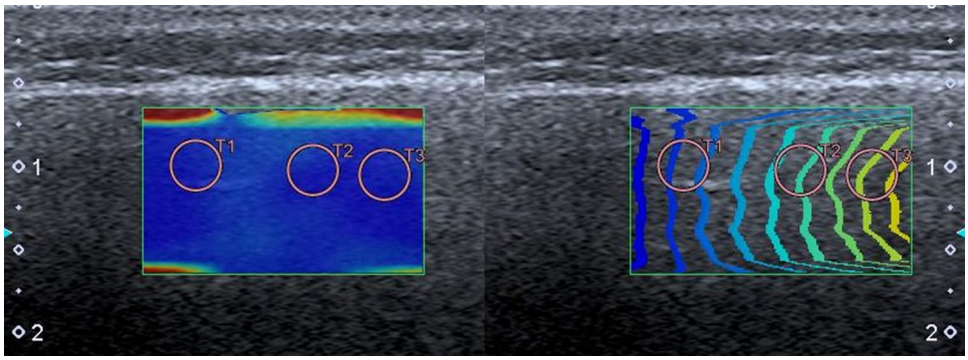

Fig. 2 Shear wave elastography measurements of the parotid gland were completed using a circular ROI that was placed on the homogeneous parenchyma. The 2D-SWE map (left side) and quality mode (right side) are shown. Three valid measurements were taken in two modes (kPa and m/s)

a mode in which reliable data are obtained when the lines are parallel and smooth, and the increase in distance between the lines is parallel to the increase in elasticity. Subsequently, a 5-mm-diameter region of interest (ROI) was used to take measurements at three different points within homogeneous parenchyma that did not contain vascular structures and lymph nodes. The mean of the measured data points was calculated. For measurements, the elasticity modulus (kPa: range 0–45) and shear wave velocity modulus (m/s: range 0–8) were used.

Doppler techniques

SMI is an innovative Doppler technique that allows visualization of very small vessels that cannot be identified by conventional Doppler methods. CD and PD use traditional wall filters to suppress background motion artifacts. This prevents imaging of low-velocity small vascular structures. SMI is an advanced application of scattering suppression to subtract flow signals with high frame rates displayed as a colored image (color SMI) or a gray-scale image of flow (monochrome SMI) [17]. In this study, to objectively visually compare with other Doppler methods, color SMI mode was used (SMI > 50 Hz frame rate vs. CD and PD with 10–15 Hz frame rates). SMI, CD, and PD were performed using a pulse repetition frequency set at 220–234 Hz and 870–966 Hz, respectively. A color-coded SMI, which shows blood flow in a color display, was used. The color gain was automatically set to 40 dB, which adequately suppressed the background color. For all cases, a fixed window with 1.5×1 cm dimensions containing homogeneous parotid parenchyma was used. Within the fixed window in the same parenchyma area, the total vascular spot counts were measured with SMI, CD, and PD (Fig. 3).

Statistical analysis

SPSS 22.0 (IBM Corporation, Armonk, New York, USA) was used for analysis of variables. The mean values for girls and boys, below and above 10 years of age, and right and left parotid gland were compared to determine their respective normal elasticity values. In the same groups, mean normal vascular spot counts were determined with SMI, CD, and PD and compared with each other. Additionally, all variables were compared with BMI. The Shapiro–Wilk test was used to assess the fit of data to a normal distribution. Comparison of quantitative data in two independent groups used the independent samples t test bootstrap results, while the Mann–Whitney *U* test Monte Carlo results were used. The Wilcoxon signed-rank test was used for dependent samples. For comparison of categorical variables, the

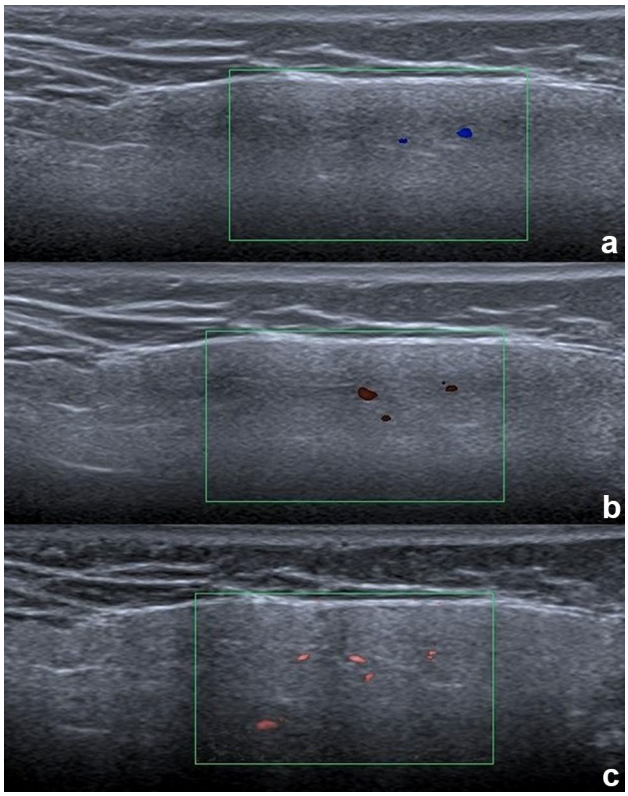

Fig. 3 Two vascular spot flows using color Doppler imaging (**a**), three vascular spot flows using power Doppler imaging (**b**), five vascular spot flows using superb microvascular imaging (**c**)

Pearson Chi-square test exact results were used. Quantitative variables are shown as mean ± standard deviation (STD) and mean/median range (maximum–minimum) in the tables. Variables were investigated at the 95% confidence interval, and *p* values below 0.05 were accepted as significant.

Results

The descriptive analysis of age, BMI as well as the elasticity (kPa) and shear wave velocity (m/s) values of the right and left parotid glands from SWE and the vascular counts from within the fixed window using SMI, CD, and PD are given in Table 1. There was no significant difference between male and female results in terms of ages above and below 10 years, age, and BMI values (Table 2). There was no significant difference between the elasticity and Doppler values for the right and left parotid gland as well as males and females (Tables 3, 4).

Using SWE, the median values for elasticity and shear wave velocity measured in both parotid glands were 8.37 ± 2.09 kPa (range 5.60–13.6) and 1.68 ± 0.26 m/s (range 1.35–2.54) on the right and 8.33 ± 2.04 kPa (range 5.50–13.9) and 1.69 ± 0.26 m/s (range 1.33–2.50) on the left. There was a significant positive correlation between the elasticity values above the age of 10 years (≥ 10) and below the age of 10 (< 10) (Fig. 4). As age increased, the elasticity values (kPa and m/s) increased (Table 5). For the right parotid gland above the age of 10 years (≥ 10), the median elasticity was 9.4 kPa and 1.81 m/s, while for the left parotid gland the median values was 9.6 kPa and 1.81 m/s. Below the age of 10 years, the median values for the right parotid gland were 7.3 kPa and 1.52 m/s and 7.4 kPa and 1.53 m/s for the left parotid gland. There was a positive significant correlation between BMI and the elasticity values ($p < 0.05$) (Table 6).

For vascularity assessment, the median values for vascular spot counts from Doppler measurements for both parotid glands were 5 ± 1.7 (range 2–9), 3.5 ± 1.45 (range 1–8), and 2 ± 1.10 (range 1–5) on the right and 4 ± 1.7 (range 2–9), 4 ± 1.43 (range 1–9), and 2 ± 1.05 (range 1–5) on the left for SMI, PD, and CD, respectively. There were no significant differences between SMI, CD, and PD for above and below the age of 10 or for right and left parotid glands ($p > 0.05$) (Table 5). There were no significant correlations between BMI with SMI, CD, and PD (Table 6). The Wilcoxon signed-rank test results revealed that the median values of spot vessels obtained by SMI were significantly higher than the median values of spot vessels obtained by both CD and PD ($p = 0.001$). Also, the median values obtained by PD were significantly higher than the median values obtained by CD ($p = 0.001$) (Fig. 5).

Table 1 Descriptive analysis of age, BMI, elasticity, and Doppler techniques

n = 100	Mean	Median	Standard deviation	Minimum	Maximum
Age	10.15	10.00	3.70	3.00	18.00
BMI	19.20	18.95	4.30	14.30	30.0
Right parotid gland					
SWE kPa	8.61	8.37	2.09	5.60	13.60
SWE m/s	1.71	1.68	0.26	1.35	2.54
SMI (*n*)	4.94	5.00	1.70	2.00	9.00
PD (*n*)	3.71	3.50	1.45	1.00	8.00
CD (*n*)	2.00	1.00	0.35	1.00	2.00
Left parotid gland					
SWE kPa	8.65	8.33	2.04	5.50	13.90
SWE m/s	1.70	1.69	0.26	1.33	2.50
SMI (*n*)	4.9	4.00	1.70	2.00	9.00
PD (*n*)	1.68	4.00	1.43	1.00	9.00
CD (*n*)	1.11	1.00	0.31	1.00	5.00

n number, *BMI* body mass index, *kPa* kiloPascals, *m/s* meters/second, *SMI* superb microvascular imaging, *PD* power Doppler, *CD* color Doppler

Table 2 The relationships between gender, age, and BMI

	Girls (*n* = 50)	Boys (*n* = 50)	Total (*n* = 100)	*p* value
< 10 (*n*)	23	26	49	0.689
≥ 10 (*n*)	27	24	51	
	Mean ± SD/Min.–Max.	Mean ± SD/Min.–Max.	Mean ± SD/Min.–Max.	
Age	10.26 ± 3.76/3–18	10.02 ± 3.76/4–18	10.14 ± 3.74/3–18	0.792
BMI	19.19 ± 3.70/12.15–28.8	19.18 ± 4.91/14.3–30.4	19.19 ± 4.33/14.3–30.4	1

Pearson's Chi-square test (Monte Carlo)/independent *t* test (bootstrap)

sd standard deviation, *Min.* minimum, *Max.* maximum, *n* number, *BMI* body mass index

Table 3 The relationship between bilateral parotid glands and gender in terms of elasticity and Doppler values

	R parotid gland (median/Min.–Max.)	*L* parotid gland (median/Min.–Max.)	*p* value
Girls			
SWE kPa	8.15 (5.60–12.80)	8.44 (5.50–13.20)	0.69
SWE m/s	1.64 (1.35–2.38)	1.70 (1.33–2.45)	0.67
SMI (*n*)	5 (2–8)	4 (2–8)	0.54
PD (*n*)	4 (1–8)	4 (1–9)	0.87
CD (*n*)	2 (1–4)	2 (1–4)	0.72
Boys			
SWE kPa	8.40 (5.60–13.60)	8.26 (5.60–13.90)	0.90
SWE m/s	1.68 (1.35–2.54)	1.66 (1.35–2.50)	0.81
SMI (*n*)	5 (3–9)	4.5 (3–9)	0.91
PD (*n*)	3 (2–7)	3 (2–7)	0.92
CD (*n*)	2 (1–5)	2 (1–5)	0.64

Mann–Whitney *U* test (Monte Carlo) Min.: Minimum/Max.: Maximum

kPa kiloPascals, *m/s* meters/second, *SMI* superb microvascular imaging, *PD* power Doppler, *CD* color Doppler

Discussion

The parotid gland is the largest saliva gland in the body and releases saliva to ease chewing and swallowing. Parotid gland diseases contain a broad range of infectious, inflammatory, autoimmune, congenital, and neoplastic disorders. In pediatric patients, the majority of parotid gland diseases comprise viral infections (e.g., mumps, CMV, and HIV), bacterial infections (e.g., staphylococcus aures, gram-positive cocci, gram-negative rods, and anaerobic bacteria), and sialadenitis [12]. In children and adults, early identification and beginning appropriate treatment is very important in terms of preventing complications like sialectasis, cervical, or supraglottic edema from spreading to other organs and abscesses. Other more rarely observed diseases in children are juvenile Sjogren syndrome, hemangiomas and vascular malformations, and lymphomas [18].

Though imaging methods like magnetic resonance imaging (MRI), computed tomography (CT), MRI sialography, and angiography may be used in the diagnosis of these diseases, ultrasound scanning is an excellent method, especially in children since it is noninvasive, comfortable, easily accessible, and free of ionizing radiation [19]. In addition to commonly observed inflammatory and infectious processes in children, neoplastic diseases change the elasticity of the parotid gland. With the classic method of palpation, the rigidity and elasticity of surficial tissues may be assessed. However, as this method is very subjective, there is a need for methods to identify more objective numerical values. Ultrasound elastography is a new method to obtain a quantitative evaluation of tissue stiffness. It can be integrated into conventional ultrasound equipment and thereby performed with gray-scale ultrasound. Gray-scale ultrasound aided by elastography methods can be used to determine benign and malignant lesions or diagnose inflammatory and infectious processes. It may also be used as a response to treatment and follow-up. Tarantino et al. [20] reported that parotid glands showed normal echotexture with multiple hypoechoic intraparenchymal lymph nodes on gray-scale ultrasound in the diagnosis of post-pubertal epidemic parotitis. We believe that elastography may also be used as a noninvasive technique to determine the early changes before the gray-scale ultrasound findings deteriorate. Future studies are necessary to establish the role of elastography in this manner.

Table 4 The relationship between gender and bilateral parotid glands in terms of elasticity and Doppler values

	Girls (median/Min.–Max.)	Boys (median/Min.–Max.)	*p* value
R parotid gland			
SWE kPa	8.15 (5.60–12.80)	8.40 (5.60–13.60)	0.84
SWE m/s	1.64 (1.35–2.38)	1.68 (1.35–2.54)	0.83
SMI (*n*)	5 (2–8)	5 (3–9)	0.85
PD (*n*)	4 (1–8)	3 (2–7)	0.76
CD (*n*)	2 (1–4)	2 (1–5)	0.79
L parotid gland			
SWE kPa	8.44 (5.50–13.20)	8.26 (5.60–13.90)	0.48
SWE m/s	1.70 (1.33–2.45)	1.66 (1.35–2.50)	0.63
SMI (*n*)	4 (2–8)	4.5 (3–9)	0.60
PD (*n*)	4 (1–9)	3 (2–7)	0.75
CD (*n*)	2 (1–4)	2 (1–5)	0.49

Mann–Whitney *U* test (Monte Carlo) Min.: Minimum/Max.: Maximum

n number, *kPa* kiloPascals, *m/s* meters/second, *SMI* superb microvascular imaging, *PD* power Doppler, *CD* color Doppler

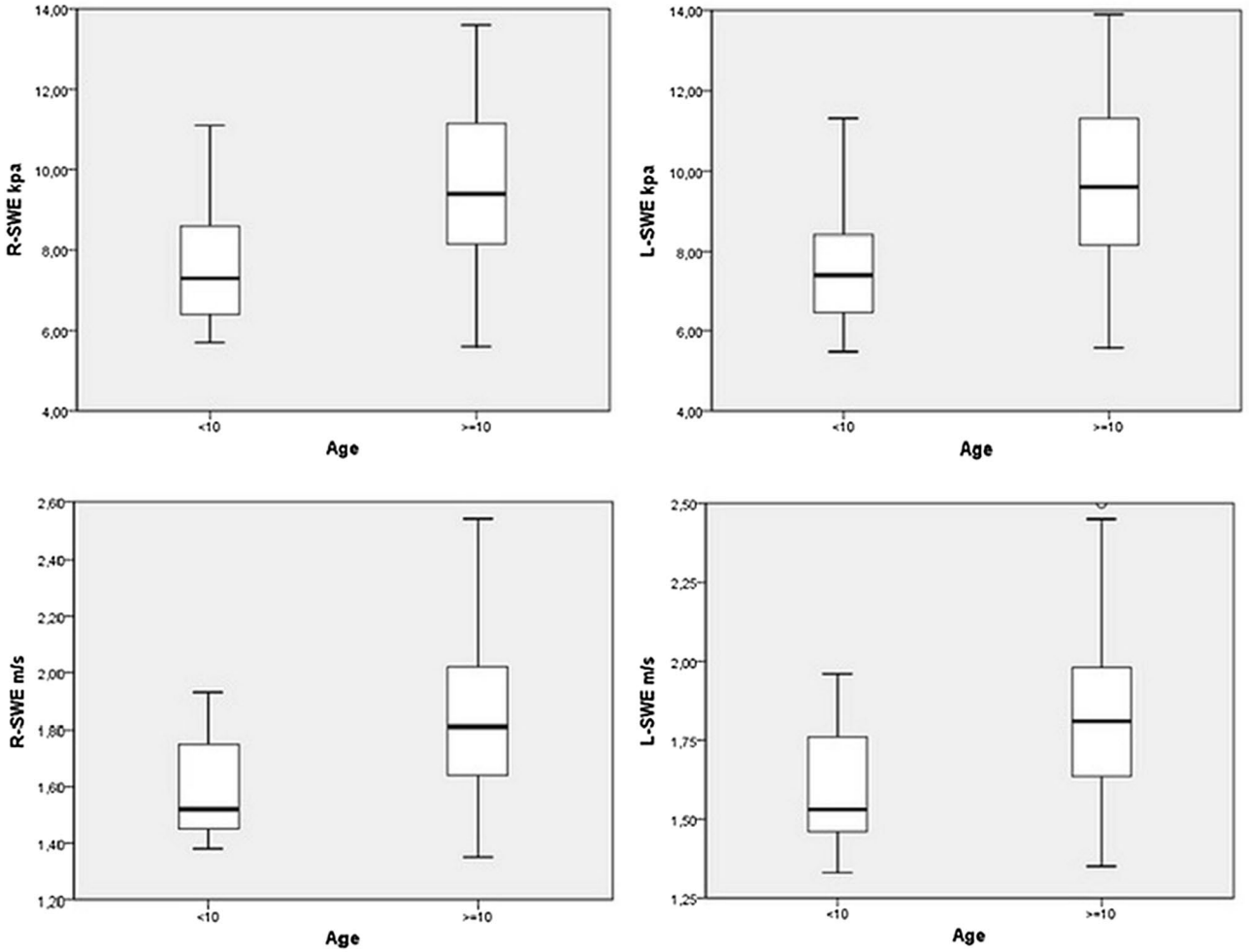

Fig. 4 Below 10 years of age (≥10), elasticity values (in kPa and m/s) significantly increased in the bilateral parotid gland compared to above 10 years (<10)

The CD mode is beneficial to identify parenchyma and mass vascularization or non-perfused cysts [12]. Doppler methods may be used to characterize hemangioma, arteriovenous malformation, or sialadenitis. SMI is a more recent method compared with elastography, and its greatest advantage is that it can show very fine vascular structures more successfully than CD and PD [21]. Normal elasticity and vascularity values for the parotid gland may help as a marker for diagnosis of infectious diseases like parotitis, inflammatory diseases like juvenile Sjogren syndrome, and neoplastic diseases like lymphoma. SWE and SMI may be helpful to assess parotid gland diseases over a wide spectrum by demonstrating ultrastructural changes that are not detected on gray-scale ultrasound. This study is unique because it investigates the normal parotid glands of children and adolescents using SWE and SMI methods.

There may be differences in the elasticity values of organs between children and adults. For example, Palabiyik et al. [3], in a study of newborns and infants, found a mean liver elasticity value of 1.70 ± 0.24 m/s and emphasized that this was higher than older children and adults. Bailey et al. [4] mentioned that multivariate linear regression demonstrated liver elasticity to be primarily associated with age in normal-weight children and with BMI in obese children. Berko et al. concluded that the elasticity of biceps brachii decreased and the elasticity of rectus femoris increased with increasing body mass index in children. Our study supports the authors that the elasticity of organs can be affected by age and BMI. In a study published by Herman et al. [8] including adults (age range 21–91 years), the normal elasticity values for the parotid gland, thyroid and submandibular glands, masseter and sternocleidomastoid muscles, and cervical lymph nodes were determined, and the mean normal elasticity value for the parotid gland was identified as 9.0 ± 3.5 kPa. The authors found a slight general decrease in elasticity with increasing age. BMI and weight had a small impact on the minimum and maximum elasticity values. But, the clinical impact of all the mentioned factors affecting

Table 5 The relationship between age and elasticity values

$n=100$	< 10 years old (median/Min.–Max.)	≥ 10 years old (median/Min.–Max.)	p value
R parotid gland			
SWE kPa	7.30 (5.70–11.10)	9.40 (5.60–13.60)	**< 0.001***
SWE m/s	1.52 (1.38–1.93)	1.81 (1.35–2.54)	**< 0.001***
SMI (*n*)	5 (2–9)	5 (2–8)	0.31
PD (*n*)	3 (1–7)	4 (1–8)	0.63
CD (*n*)	2 (1–5)	2 (1–5)	0.19
L parotid gland			
SWE kPa	7.40 (5.5–11.30)	9.60 (5.60–13.90)	**< 0.001***
SWE m/s	1.53 (1.33–1.96)	1.81 (1.35–2.50)	**< 0.001***
SMI (*n*)	4 (2–9)	5 (2–9)	0.31
PD (*n*)	3 (1–7)	4 (1–9)	0.42
CD (*n*)	2 (1–5)	2 (1–5)	0.38

Mann–Whitney *U* test (Monte Carlo) Min.: Minimum/Max.: Maximum

Bold values depict the level of significance

n number, *kPa* kiloPascals, *m/s* meters/second, *SMI* superb microvascular imaging, *PD* power Doppler, *CD* color Doppler

*Significant correlation ($p < 0.05$)

Table 6 Correlation analysis between bilateral parotid glands and BMI

	BMI	
	r	*p*
R parotid gland		
SWE kPa	0.18	**0.007***
SWE m/s	0.16	**0.017***
SMI (*n*)	0.07	0.311
PD (*n*)	0.07	0.308
CD (*n*)	0.02	0.711
L parotid gland		
SWE kPa	0.23	**0.001***
SWE m/s	0.19	**0.005***
SMI (*n*)	0.01	0.836
PD (*n*)	0.05	0.520
CD (*n*)	0.006	0.942

Kendall's tau *b* correlation test, *r* correlation coefficient

Bold values depict the level of significance

n number, *kPa* kiloPascals, *m/s* meters/second, *SMI* superb microvascular imaging, *PD* power Doppler, *CD* color Doppler

*Significant correlation ($p < 0.05$)

elasticity is probably minimal. Contrary to this, elasticity for parotid glands is affected by age and BMI according to our study. In general, the pediatric population should be considered separately from adults. The pediatric population are exposed to many hormonal and biological changes in the

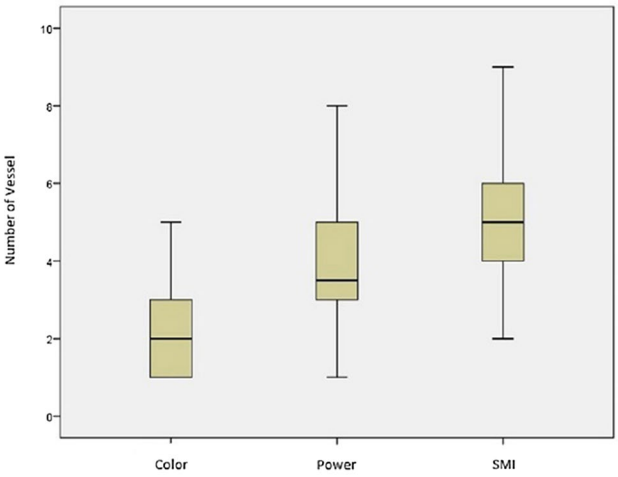

Fig. 5 The median number of vascular spots obtained by superb microvascular imaging was significantly higher than the median number of vascular spots obtained by both color Doppler imaging and power Doppler imaging

transition from childhood (under 10 years) to adolescence (above 10 years). The elasticity of the organs in children and adolescents may be more susceptible to age and BMI changes than adults. The different results between studies may be related with this situation. Mantsopoulos et al. [9], in a study of 25 healthy adults, found that the normal SWE elasticity value of the parotid gland was 1.85 m/s. Compared with this study, the elasticity value for the parotid gland in children was minimally lower in both kPa and m/s mode. In the present study, the ultrasound device used was able to obtain elasticity values in both kPa and m/s. In this way, our study has an advantage compared to these previous studies. Gungor et al. [10], in a study using the SE elastography method on a total of 54 children, determined the normal strain index value for the parotid gland and found no significant difference between male and female children, age, and BMI. Similar to this study, our study found no significant difference between elasticity values in terms of sex. However, there were significant positive correlations between age and BMI. The cause of this difference may be due to the use of different elastography methods. Moreover, the higher number of patients in our study may have changed the statistics and results.

Identification of increased vascular flow in soft tissues is accepted as showing active inflammation and parenchymal remodeling in the parotid gland, as in other organs [22–24]. Shimizu et al. [22] determined increased vascularity of the parotid gland and 4–6 vascular spot contents on CD with Sjogren syndrome. Martinoli et al. [23] reported that vascularization in the parotid gland increased due to benign lymphoepithelial lesions in HIV infections, and mixed nodules were more hypervascular compared to cyst-like

nodules. Additionally, Fischer et al. [24] identified increased parenchymal vascularity on CD and PD with parotid gland sarcoidosis (Heerfordt's syndrome). Conventional CD does not clearly detect fine and slow-velocity blood flow. Developments in ultrasound Doppler technology have increased its sensitivity and spatial resolution. PD is an integrated power spectrum that depends on low angle and has higher sensitivity in detecting the low blood flow velocity. In contrast, CD is based on the mean Doppler frequency shift [25, 26]. Due to the developed filtering technique in SMI, background noises are eliminated, and small slow-velocity vascular structures may be successfully imaged. Compared with standard PD, SMI has high sensitivity and resolution [21]. Indeed, in the present study, SMI was found to be superior to CD and PD in identifying parotid gland vascularity. Higher numbers of fine vascular spots were observed that could not be seen on CD and PD. Within a fixed window with 1.5×1 cm dimensions, SMI imaged 5 ± 1.70 vascular spots in the right parotid gland and 4 ± 1.70 vascular spots in the left parotid gland. The basal vascularity values for children found in this preliminary study may be beneficial in terms of identifying sialadenitis, autoimmune, and neoplastic diseases.

Among the limitations of our study are the low number of patients, the exclusion of children younger than 3 years of age, counting of vascular structures within a fixed window instead of the whole surface of the parotid lobe, and a lack of deep-lobe measurements.

Conclusion

This preliminary study determined the reference SWE, SMI, PD, and CD values for the parotid gland in pediatric patients. The normal values may be used to differentiate benign and malignant lesions and diagnose inflammatory and infectious processes. The elasticity values displayed variations linked to age and BMI, but vascularity values were not affected by age, sex, and BMI. SMI is a new method that can provide more detailed information about vascularity compared with other methods.

Acknowledgements We acknowledge Ms. Manolya Kara Acar in assisting to review the publications and Ms. Yeliz Pekcevik for her assistance in the online literature search.

Compliance with ethical standards

Conflict of interest The authors declare that they have no conflicts of interest.

Ethical approval The institutional review board approved the study and waived the need for patient consent.

References

1. Hu X, Liu Y, Qian L (2017) Diagnostic potential of real-time elastography (RTE) and shear wave elastography (SWE) to differentiate benign and malignant thyroid nodules: a systematic review and meta-analysis. Medicine (Baltimore) 96:e8282. https://doi.org/10.1097/MD.0000000000008282
2. Mulazzani L, Salvatore V, Ravaioli F et al (2017) Point shear wave ultrasound elastography with Esaote compared to real-time 2D shear wave elastography with supersonic imagine for the quantification of liver stiffness. J Ultrasound 20:213–225. https://doi.org/10.1007/s40477-017-0260-7
3. Palabiyik FB, Inci E, Turkay R, Bas D (2017) Evaluation of liver, kidney, and spleen elasticity in healthy newborns and infants using shear wave elastography. J Ultrasound Med 36:2039–2045. https://doi.org/10.1002/jum.14202
4. Bailey SS, Youssfi M, Patel M, Hu HH, Shaibi GQ, Towbin RB (2017) Shear-wave ultrasound elastography of the liver in normal-weight and obese children. Acta Radiol 58:1511–1518. https://doi.org/10.1177/0284185117695668
5. Ren WW, Li XL, He YP et al (2017) Two-dimensional shear wave elastography of breast lesions: comparison of two different systems. Clin Hemorheol Microcirc 66:37–46. https://doi.org/10.3233/CH-16243
6. Aksoy S, Colak C, Nalbant MO, Turkay R, Erdil I, Hocaoglu E, Inci E, Alis H (2017) Comparison of elasticity values of the right lobe of the liver of normal weight and morbidly obese Turkish patients. Niger J Clin Pract 20:542–544. https://doi.org/10.4103/1119-3077.206362
7. Leung WKC, Chu KL, Lai C (2017) Sonographic evaluation of the immediate effects of eccentric heel drop exercise on Achilles tendon and gastrocnemius muscle stiffness using shear wave elastography. PeerJ 19:e3592. https://doi.org/10.7717/peerj.3592
8. Herman J, Sedlackova Z, Vachutka J, Furst T, Salzman R, Vomacka J (2017) Shear wave elastography parameters of normal soft tissues of the neck. Biomed Pap Med Fac Univ Palacky Olomouc Czech Repub 161:320–325. https://doi.org/10.5507/bp.2017.024
9. Mantsopoulos K, Klintworth N, Iro H, Bozzato A (2015) Applicability of shear wave elastography of the major salivary glands: values in healthy patients and effects of gender, smoking and pre-compression. Ultrasound Med Biol 41:2310–2318. https://doi.org/10.1016/j.ultrasmedbio.2015.04.015
10. Gungor G, Yurttutan N, Bilal N, Menzilcioglu MS, Duymus M, Avcu S, Citil S (2016) Evaluation of parotid glands with real-time ultrasound elastography in children. J Ultrasound Med 35:611–615. https://doi.org/10.7863/ultra.15.03073
11. Katz P, Hartl DM, Guerre A (2009) Clinical ultrasound of the salivary glands. Otolaryngol Clin North Am 42:973–1000. https://doi.org/10.1016/j.otc.2009.08.009
12. Iro H, Zenk J (2014) Salivary gland diseases in childhood. Laryngorhinootologie 93:103–125. https://doi.org/10.3205/cto000109
13. Demené C, Deffieux T, Pernot M et al (2015) Spatiotemporal clutter filtering of ultrafast ultrasound data highly increases Doppler and fUltrasound sensitivity. IEEE Trans Med Imaging 34:2271–2285. https://doi.org/10.1109/TMI.2015.2428634
14. Ohno Y, Fujimoto T, Shibata Y (2017) A new era in diagnostic ultrasound, superb microvascular imaging: preliminary results in pediatric hepato-gastrointestinal disorders. Eur J Pediatr Surg 27:20–25. https://doi.org/10.1055/s-0036-1593381
15. Kim HK, O'Hara S, Je BK, Kraus SJ, Horn P (2017) Feasibility of superb microvascular imaging to detect high-grade vesicoureteral reflux in children with urinary tract infection. Eur Radiol. https://doi.org/10.1007/s00330-017-4974-x

16. Lee YS, Kim MJ, Han SW, Lee HS, Im YJ, Shin HJ, Lee MJ (2016) Superb microvascular imaging for the detection of parenchymal perfusion in normal and undescended testes in young children. Eur J Radiol 85:649–656. https://doi.org/10.1016/j.ejrad.2015.12.023
17. Machado P, Segal S, Lyshchik A, Forsberg F (2016) A novel microvascular flow technique: initial results in thyroids. Ultrasound Q 32:67–74. https://doi.org/10.1097/RUQ.0000000000000156
18. Carlson ER, Ord RA (2016) Benign pediatric salivary gland lesions. Oral Maxillofac Surg Clin 28:67–81. https://doi.org/10.1016/j.coms.2015.07.004
19. Rastogi R, Bhargava S, Mallarajapatna GJ, Singh SK (2012) Pictorial essay: salivary gland imaging. Indian J Radiol Imaging 22:325–333. https://doi.org/10.4103/0971-3026.111487
20. Tarantino L, Giorgio A, De Stefano G, Farella N (2000) Ultrasonography in the diagnosis of post-pubertal epidemic parotitis and its complications. Radiol Med 99:461–464
21. Zhan J, Diao XH, Jin JM, Chen L, Chen Y (2016) Superb microvascular imaging—a new vascular detecting ultrasonographic technique for avascular breast masses: a preliminary study. Eur J Radiol 85:915–921. https://doi.org/10.1016/j.ejrad.2015.12.011
22 Shimizu M, Okamura K, Yoshiura K, Ohyama Y, Nakamura S (2008) Sonographic diagnosis of Sjögren syndrome: evaluation of parotid gland vascularity as a diagnostic tool. Oral Surg Oral Med Oral Pathol Oral Radiol Endod 106:587–594. https://doi.org/10.1016/j.tripleo.2007.11.007
23 Martinoli C, Pretolesi F, Del Bono V, Derchi LE, Mecca D, Chiaramondia M (1995) Benign lymphoepithelial parotid lesions in HIV-positive patients: spectrum of findings at gray-scale and Doppler sonography. AJR Am J Roentgenol 165:975–979. https://doi.org/10.2214/ajr.165.4.7677004
24 Fischer T, Mühler M, Beyersdorff D, Guski H, Bollow M, Hamm B, Werbs M, Filimonow S (2003) Use of state-of-the-art ultrasound techniques in diagnosing sarcoidosis of the salivary glands (Heerfordt's syndrome). HNO 51:394–399. https://doi.org/10.1007/s00106-002-0717-6
25 Choi BI, Kim TK, Han JK, Chung JW, Park JH, Han MC (1996) Power versus conventional color Doppler sonography: comparison in the depiction of vasculature in liver tumors. Radiology 200:55–58. https://doi.org/10.1148/radiology.200.1.8657945
26 Kwak JY, Kim EK, Kim MJ, Choi SH, Son E, Oh KK (2008) Power Doppler sonography: evaluation of solid breast lesions and correlation with lymph node metastasis. Clin Imaging 32:167–171. https://doi.org/10.1016/j.clinimag.2007.12.004